Supporting Information

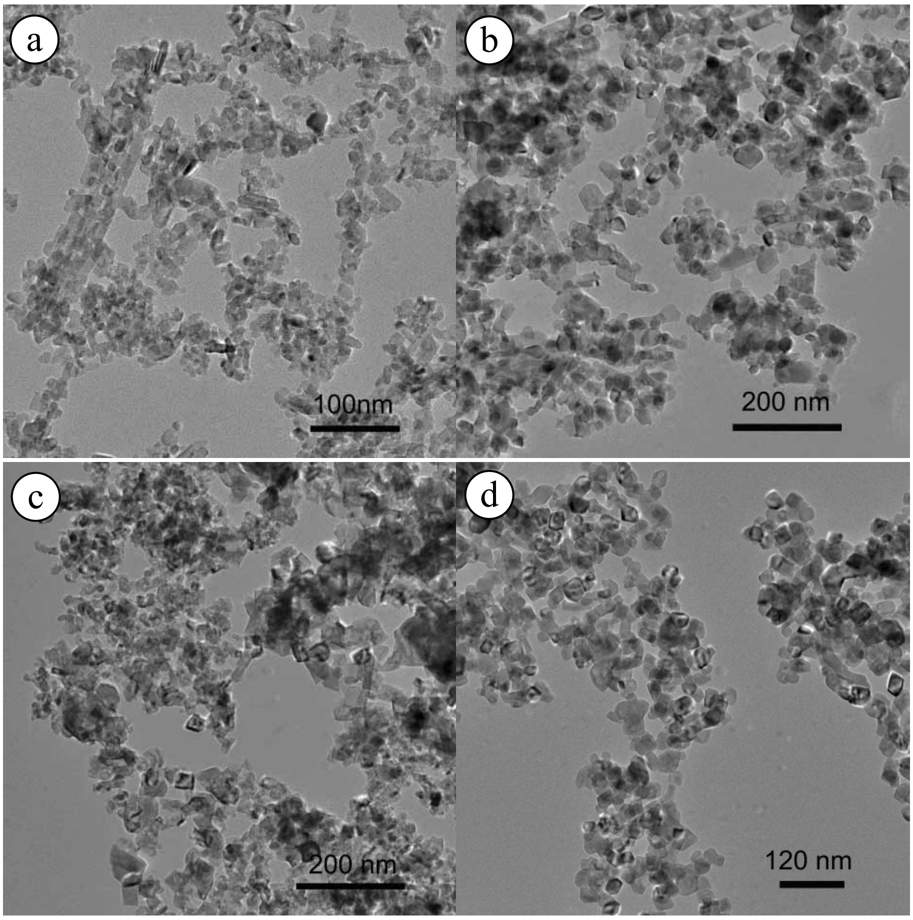

Figure S1. TEM pictures of (a) N-NTA (600), (b) N-NTA (700), (c) N-NTA (800), and (d) N- TiN.

Figure S1 shows the TEM micrographs of N-NTA nano-powders prepared at different temperatures. After treatment under an NH_3 flow at T = 600~700 ^oC for 4 h, the nanotubular morphology of NTA is broken and converted into nanobundles ((a) and (b)). After treatment under an NH_3 flow at T = 800~900 ^oC for 4 h ((c) and (d)), nanoparticles with loose agglomerate are harvested.

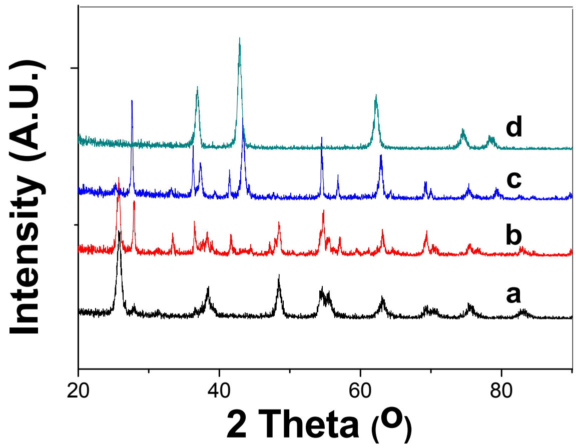

Figure S2. XRD patterns of (a) N- NTA (600), (b) N- NTA (700), (c) N-NTA (800), and (d) N-TiN.

The effect of the nitridation temperature on the powder phase composition is clearly illustrated in Figure S2. N-doped TiO_2 (anatase) is obtained by treating NTA in an NH_3 flow at $T = 600$ ^oC. At the same time, NTA calcinated in NH_3 flow at 700~800 ^oC shows a low intensity of (101) XRD peak of anatase and new XRD peaks of TiN phase (JCPDS card No. 38-1420); and the one calcinated in flowing NH_3 at 900 ^oC shows only XRD signal of TiN phase.

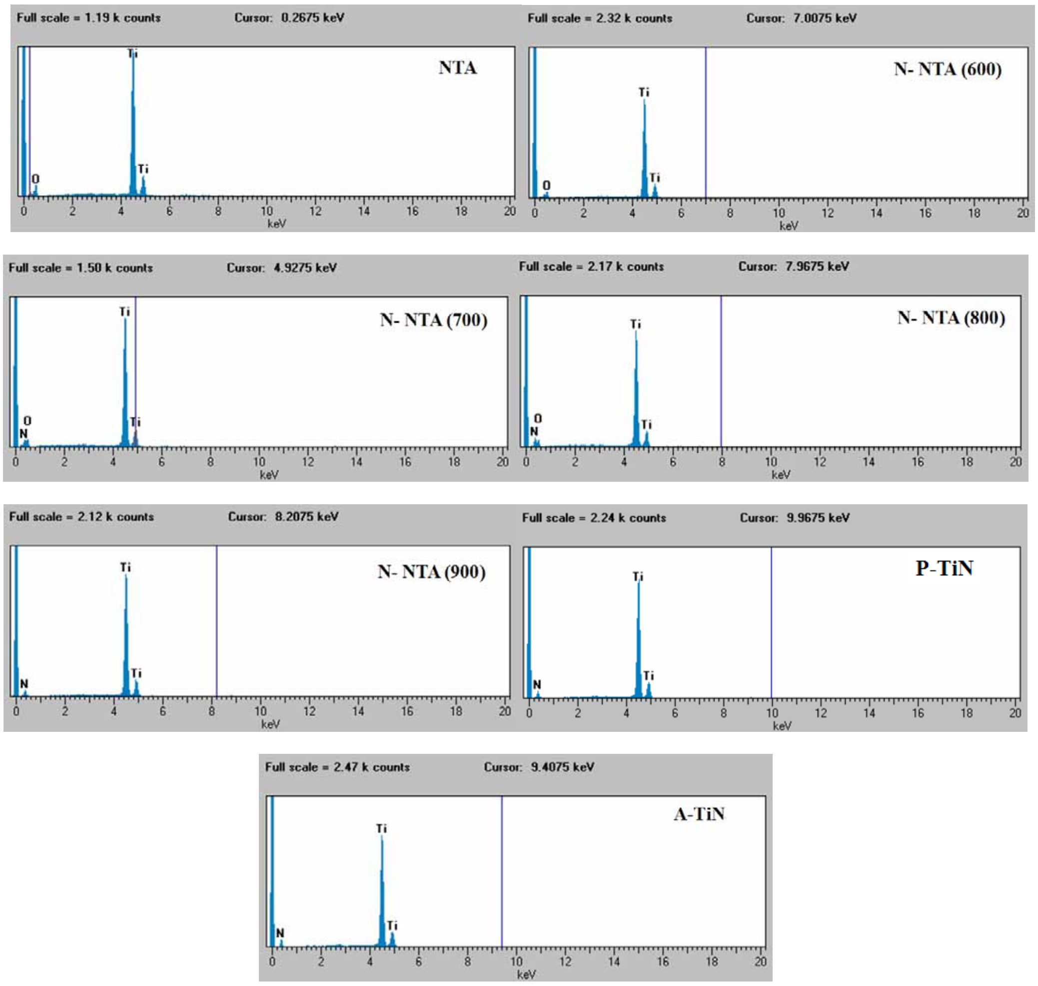

Figure S3. EDS spectra of NTA, N- NTA (600-900), P-TiN and A-TiN.

Figure S3 shows the main constituent elements (determined by EDS) of NTA, N-NTA (600-900) obtained at different temperatures and A-TiN. Only Ti and O are detected by EDS in NTA and N-NTA (600). When NTA is calcinated in NH_3 flow at 700~800 ^{o}C, Ti, N, and O elements are detected in resultant N-NTA products. Only Ti and N are detected by EDS in N-TiN obtained at 900 ^{o}C, the same as P-TiN and A-TiN.

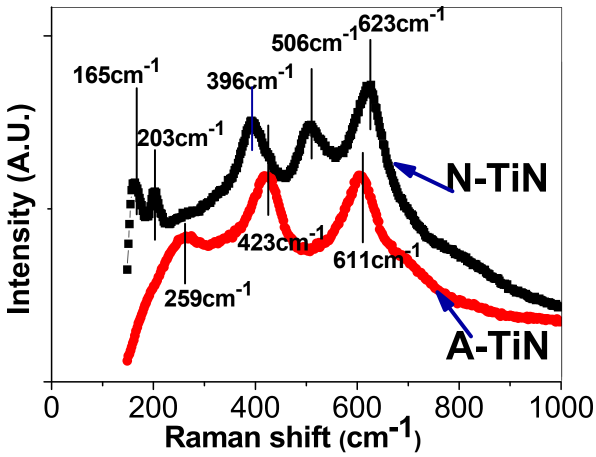

Figure S4. Raman spectra of as-prepared N-TiN and A-TiN.

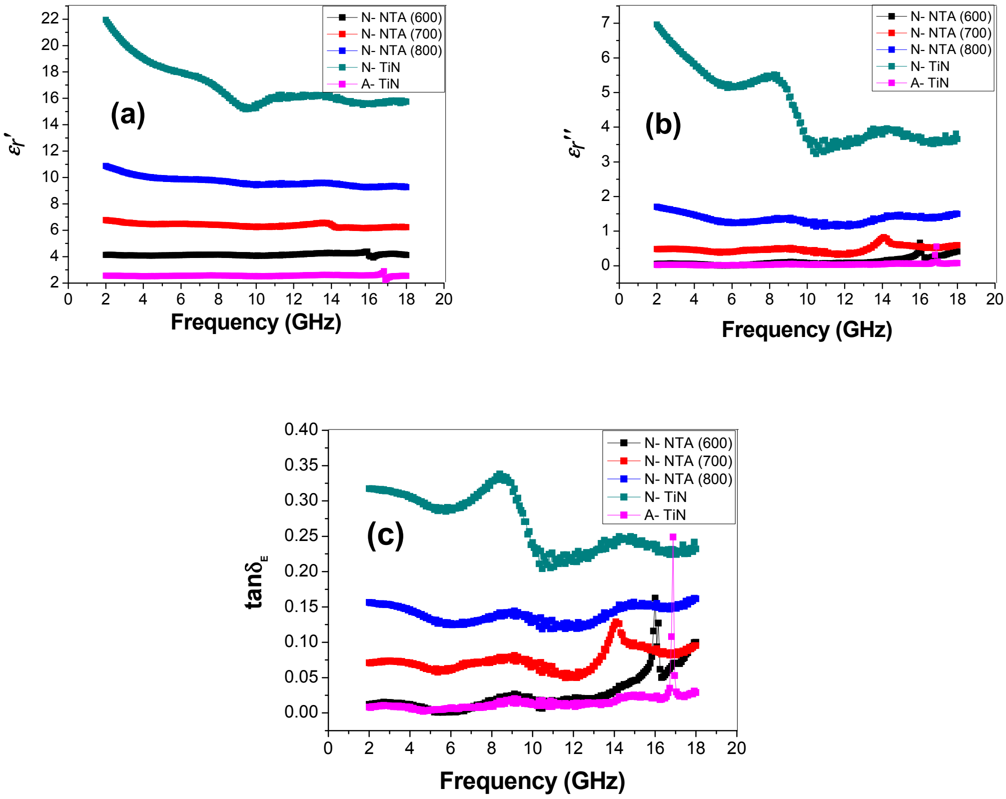

Figure S5. Real (ε_r') (a) and imaginary (ε_r'') (b) parts of the relative complex permittivity and dielectric loss ($\tan\delta_E$) (c) of N-NTA (600-900) and A-TiN filled paraffin composites in the frequency range of 2-18 GHz.

Figure S5 illustrates the real (ε_r'), imaginary parts (ε_r'') of the relative complex dielectric permittivity and dissipation factors versus frequency of the prepared N-NTA (600-900) and A-TiN imbedded in the paraffin wax composites versus the frequency. The ε_r'□ and ε_r''□□ of A-TiN are very little and almost constant with nearly no variation throughout the whole frequency range, which has a very low dielectric loss at gigahertz frequency and the $\tan\delta_E$ is limited at about 17 GHz, which means that the A-TiN is a typical dielectric material. The ε_r'□□□□, ε_r'' and $\tan\delta_E$ of N-TiN (700-900) powder composite powder are all higher than those of A-TiN evidently.